

Hierarchical Assembly of Nanostructured Organosilicate Networks via Stereocomplexation of Block Copolymers

Sung Ho Kim,[†] Fredrik Nederberg,^{†‡} Lei Zhang,[†] Charles G. Wade,[†]
Robert M. Waymouth,[‡] and James L. Hedrick^{*,†}

IBM Almaden Research Center, 650 Harry Road, San Jose, California 95120, and
Department of Chemistry, Stanford University, Stanford, California 94305

Received October 17, 2007; Revised Manuscript Received November 30, 2007

ABSTRACT

The effect of the stereochemistry of polylactide (PLA)-based block copolymers on templated inorganic nanostructures has been investigated from the self-assembly of a stereoisomer pair/organosilicate mixture followed by organosilicate vitrification and copolymer thermolysis. Isomeric PLA homopolymers, block copolymers, and a stereoblock copolymer were prepared by ring-opening polymerization of D-, L-, or *rac*-lactide using an organocatalytic catalyst. Both differential scanning calorimetry and atomic force microscopy showed the formation of a stereocomplex between enantiomeric stereoisomers, that is, block copolymer/block copolymer and block copolymer/homopolymer mixtures as well as a stereoblock copolymer. The unique noncovalent interactions driven by stereocomplexation of D- and L-lactide provided supramolecular structures with a hierarchical order as characterized by distinctive vertical and horizontal growth of toroidal nanostructured inorganic features. This study demonstrates the potential of hierarchically assembling suprastructures that bridge the nano- to mesoscale feature sizes in the design of tunable functional nanomaterials suitable for future applications of microelectronics, material science, and bioengineering.

The self-assembly of amphiphilic block copolymers in selective solvents provides a defined methodology for a variety of supramolecular assemblies including spherical micelles, worm micelles, vesicles, multicompartiment micelles, toroids, and helices.^{1–6} This versatility has attracted an increasing interest in applications in materials science, microelectronics, bioengineering, and the pharmaceutical industry.^{7–10} The need for custom materials with a defined structure and properties for the specific applications is of great interest. Traditionally, it has been achieved by the (i) design of new block copolymers (block types, chain lengths, and chain architectures), (ii) selection of solvents (solvents selective to one block), and (iii) use of additives (i.e., bases, acids, salts, and surfactants).^{11–15} However, these methods vary widely in applicability and efficiency and often require supplementary breakthroughs to develop new assembled morphologies or manipulate existing morphologies. The objective of the present study is to survey the possibility of polymer–polymer stereocomplex formation as a noncovalent driving force to control higher-order structure and expand the scope of possible morphologies from block copolymers.

Well-studied examples of polymer–polymer complexation include (i) a polyelectrolyte complex between a polyanion and polycation, (ii) a hydrogen-bonding complex between a poly(carboxylic acid) and a polyether or polyol, (iii) a charge-transfer complex between a polymeric donor and acceptor, and (iv) a complex formation between individual enantiomers with different steric structures.^{16–19} Typical examples of iso- and syndiotactic stereocomplexes are poly(methyl methacrylate), polythiiranes, polyoxiranes, polylactones, and polylactides (PLA).²⁰

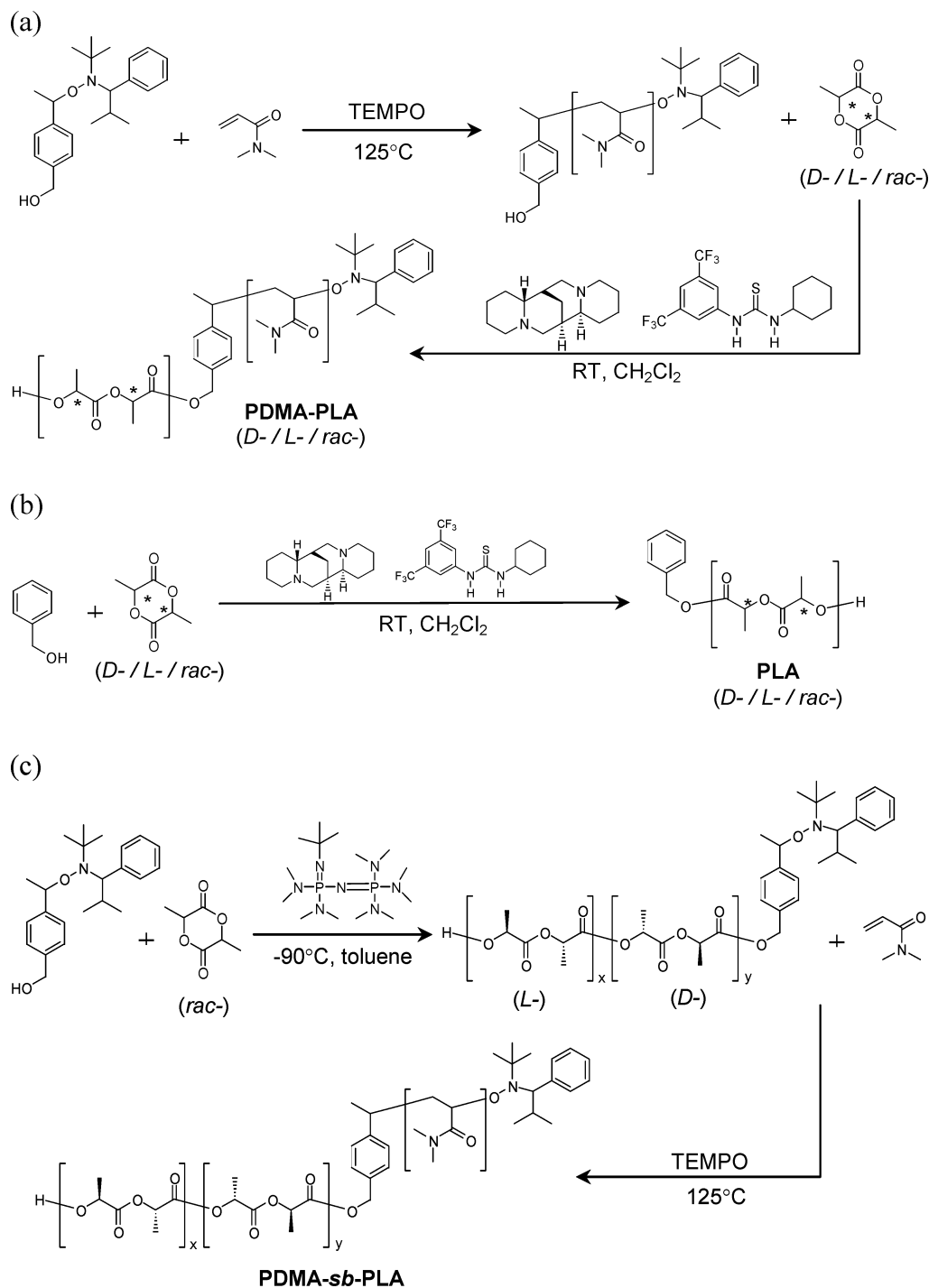
PLAs have attracted a great deal of attention because the PLA homo- and block copolymers are biodegradable, producible from renewable resources, and nontoxic to the human body and the environment, with potential use in medicine and bioengineering.^{20–24} In nanotechnology, PLA block copolymers have been used to template organosilicate vitrification and ultimately nanoporous polymeric materials.^{25,26} Since lactide monomers have two stereoisomers, L- and D-compounds, there are three types of polylactides, optically active poly(L-(–)-*S*-lactide) (L-PLA) and poly(D-(+)-*R*-lactide) (D-PLA) and racemic poly(DL-lactide) (*rac*-PLA). Since Ikada et al. first reported a stereocomplex formation from mixtures of L-PLA and D-PLA in both the melt and solution, numerous studies have been performed on the formation of the stereocomplex and its crystalline

* To whom correspondence should be addressed. Tel: 408-927-1632.
Fax: 408-927-3310. E-mail: Hedrick@almaden.ibm.com.

[†] IBM Almaden Research Center.

[‡] Stanford University.

Scheme 1. Synthesis of (a) Stereoregular Block Copolymers (PDMA–PLA), (b) Homopolymers (PLA), and (c) Stereoblock Copolymers (PDMA-*sb*-PLA)



structure, morphology, and physical structure.^{19,27–31} For example, Sarasua et al. demonstrated that the complex formation stems from a H-bonding force from specific CH₃⋯O=C and C₆H₅⋯O=C interactions between both stereoisomers of polylactide from a combined study with FT-IR spectroscopy and molecular modeling.²⁸ Kang et al. showed that stereocomplex block copolymer micelles with enhanced stability have the potential for the delivery of drugs.²⁹ Sun et al. observed thermal history-dependent phase transitions from a multilamellar vesicle to a lamellar to a honeycomb morphology in an incompatible blend of enan-

tiomeric PLA block copolymers, which may be attributed to the formation and melting of stereocomplexes.^{30,31}

In our previous work, we showed that inorganic nanostructures with widely different morphologies ranging from toroids to linear wormlike features to densely packed toroids to contiguous nanoporous monolayers could be formed from the coassembly of an amphiphilic poly(*N,N*-dimethylacrylamide-*block-rac*-lactide) copolymer (PDMA-*rac*-PLA) with a cross-linkable organosilicate precursor.^{32,33} The PDMA block has characteristics commensurate with the formation of miscible blends with organosilicate, that is, polarity,

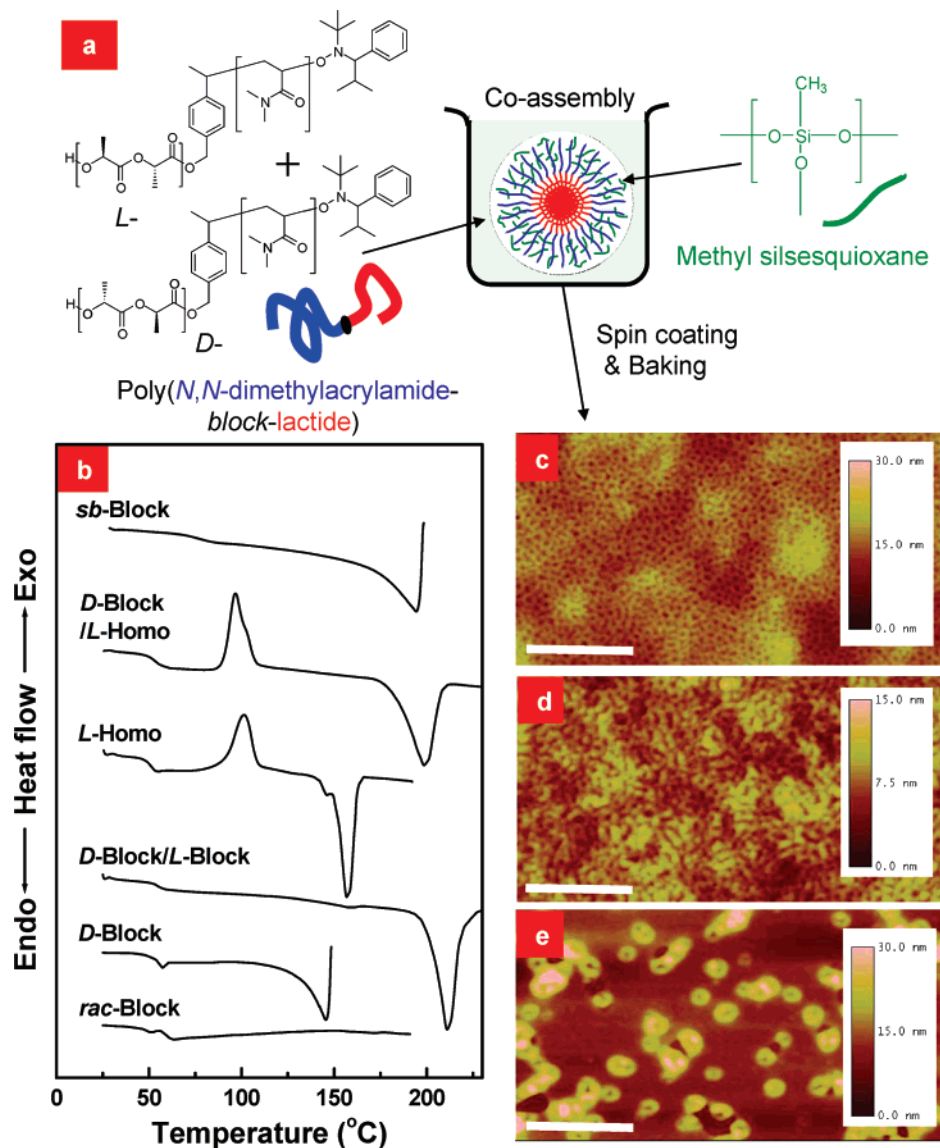


Figure 1. Stereo-controlled block copolymers and coassembled organosilicate nanostructures. (a) The nanostructures are prepared from coassembly of block copolymers and the organosilicate (OS) precursor followed by organosilicate vitrification and copolymer thermolysis. (b) DSC thermograms of precipitates from a dilute solution of block copolymers show the stereocomplexation in the mixture of enantiomeric pairs. AFM images shows three distinct morphologies formed by the mixture of enantiomeric block copolymers: (c) a contiguous nanoporous film (at 2 wt %, polymer/OS = 6/4), (d) linear features (at 1 wt %, polymer/OS = 4/6), and (e) isolated toroids (at 0.05 wt %, polymer/OS = 6/4). The scale bars are 500 nm (c–e).

hydrogen-bonding capability, and basicity, which promote strong interactions between the thermosetting organosilicate precursors and the PLA block copolymer.^{34–36} The use of PLA stems from its incompatibility with the organosilicate and thermal instability, generating porous inorganic nanostructures upon thermolysis of the copolymer. Here, we investigate the effect of stereochemistry on the resulting morphologies of an organosilicate nanostructure using the stereo-controlled block copolymers and stereocomplexation as a noncovalent structure-directing agent.

The effect of stereocomplex formation on the supramolecular morphologies was investigated using three combinations of stereoisomer pairs, (i) mixtures of PDMA–PLA block copolymers having a different stereochemistry of the lactide blocks, (ii) mixtures of an enantiomerically pure PDMA–PLA block copolymer with a PLA homopolymer

of opposite configuration, and (iii) stereoblock copolymers (PDMA-*sb*-PLA) having both the stereoregular D- and L-block in the same chain. The PLA block copolymers and homopolymers were synthesized by the ring-opening polymerization (ROP) of lactide monomers, in which the stereosequence of the resulting polylactide was governed by the optical purity of lactide monomers.^{21,37,38} Scheme 1 shows the synthesis of the block copolymers, homopolymers, and stereoblock copolymer. The ring-opening of enantiomeric lactides was performed in a glovebox using thiourea and tertiary amine catalysts designed for bifunctional activation of both the monomer and alcohol through hydrogen bonding. The utility of this catalytic system was demonstrated through the synthesis of narrowly dispersed PLA blocks with predictable molecular weights.³³ PDMA₇₀–PLA₁₅₀ block copolymers were prepared from a dual-headed initiator

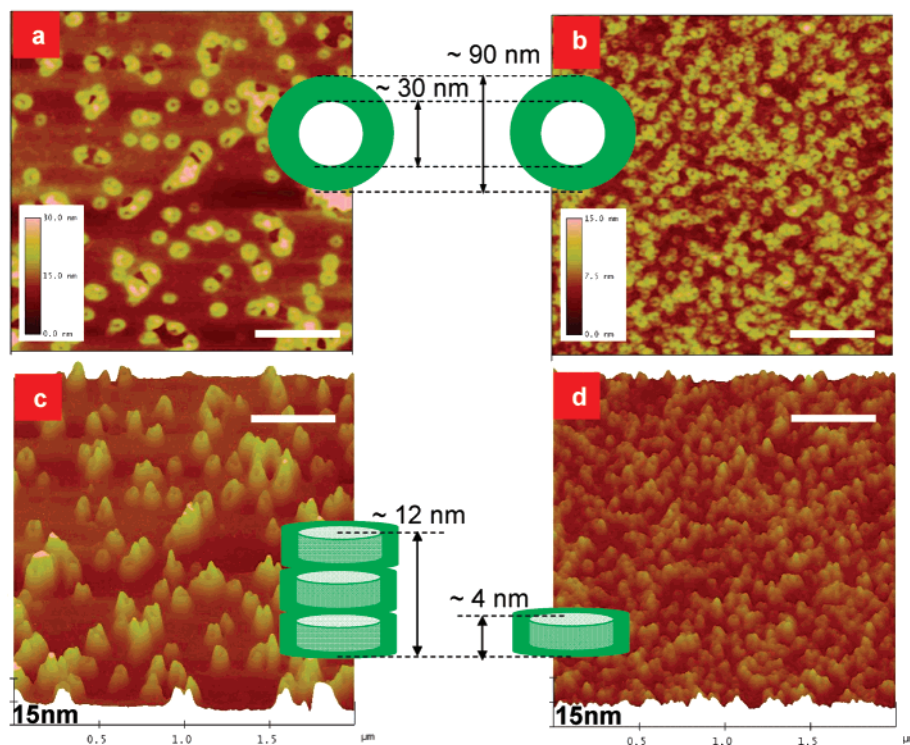


Figure 2. Top-view and side-view AFM images of toroids prepared from a 0.05 wt % dichloroethane/propylene glycol propyl ether (PGPE) solution of (D-block + L-block)/OS (60/40) (a,c) and *rac*-block/OS (60/40) (b,d). The height of toroids from the enantiomeric mixture increases (3 \times) without a significant change in diameter, compared with those from the racemate. The scale bars are 500 nm.

containing an alkoxyamine and a primary hydroxyl group through nitroxide-mediated polymerization of dimethylacrylamide and subsequent ring-opening of lactide monomers with a high optical purity.^{33,39} PLA₁₅₀ homopolymers were prepared using benzyl alcohol as an initiator. According to the enantiomer of lactide used, that is, D-lactide, L-lactide, or *rac*-lactide, the block copolymers and homopolymers are referred to as the D-/L-/*rac*-block and D-/L-/*rac*-homo, respectively. The synthesis of PDMA-*sb*-PLA stereoblock copolymers was carried out by the ROP of *rac*-lactide using 1-*tert*-butyl-2,2,4,4,4-pentakis(dimethylamino)-2 Λ^5 ,4 Λ^5 -catenadi(phosphazene) (P₂-*t*-Bu) at -90 °C.⁴⁰ The degree of isotactic enrichment of the prepared polymer was determined to be 0.95 by homonuclear decoupled ¹H NMR (see Figure S1 of Supporting information). It has been reported by Yui et al. that a stereoblock copolymer such as PLLA-*b*-PDLA easily forms a stereocomplex because of the neighboring effect of the two blocks in the copolymer.⁴¹ Full details on the synthesis and characterization of these PLA block copolymers and homopolymers are described in the Supporting Information.

Figure 1 illustrates the general procedure to produce nanostructured organosilicate thin films and the evaluation of their resulting morphologies. Differential scanning calorimetry (DSC) was used to confirm the formation of stereocomplexes prepared by precipitating dilute mixed solutions of enantiomeric polylactides without organosilicate. The DSC traces of Figure 1b show that the stereoregular copolymers are semicrystalline and manifest a T_m (~150 °C), while *rac*-lactide and the *rac*-block copolymer did not show any evidence of crystallization, only a T_g at ~55 °C. The

mixtures of L- and D-lactide block copolymers prepared from our catalyst showed a T_m of ~210 °C, significantly higher than the respective polymers (~150 °C), which is consistent with the literature values of the stereocomplex.⁴² Interestingly, the mixture of the block D and homopolymer L manifested a melting point of 200 °C, consistent with the formation of a stereocomplex and a microphase-separated morphology. Similarly, the stereoblock copolymer also showed evidence of a stereocomplex with a melting point of 200 °C. Hillmyer and others reported that the PDMA/PLA block copolymers are miscible, presumably stemming from acid–base interactions.²⁶ Similarly, the block copolymers prepared from *rac*, L, or D all manifested a single T_g with the PDMA block. However, the formation of the stereocomplex appears to outweigh the acid–base interactions facilitating phase separation in the block copolymer.

Stereocomplex formation and crystallization of isotactic stereoisomers are characterized by distinctive physical and chemical stability, accompanying the change of their solubility in specific solvents compared to that of the racemic analogue. The polymers and the inorganic precursor of methyl silsesquioxane (MSSQ) were dissolved in mixtures of dichloroethane (DCE) and propylene glycol propyl ether (PGPE). Thin films containing the block copolymer (and/or homopolymer), MSSQ, and triethylamine, a known catalyst to facilitate the silanol condensation reaction,^{35,36} were prepared by spin casting the solution on silicon wafers followed by organosilicate vitrification and copolymer thermolysis. The morphology of block copolymer/organosilicate thin films was characterized with atomic force microscopy (AFM) in the tapping mode. Height-contrast images of the

Table 1. Average Height and Surface Coverage of Organosilicate Nanostructures

sample		average height (nm)	surface coverage (%)
block only	D-block + L-block	12.8 ± 4.3	26.6
	<i>rac</i> -block	3.9 ± 1.1	83.2
block + homo	D-block + L-homo	35.0 ± 8.0	40.0
	<i>rac</i> -block + <i>rac</i> -homo	5.6 ± 1.4	82.8
variable conc.	0.5 wt %	9.3 ± 3.9	30.0
	1.0 wt %	11.3 ± 4.7	30.9
	1.5 wt %	11.4 ± 4.0	25.6
	2.0 wt %	27.6 ± 8.2	18.3
<i>sb</i> -block	high <i>C</i>	$2.8 \pm 1.7/$ 4.5 ± 2.7	83.0
	low <i>C</i>	3.9 ± 1.1	33.2
	<i>sb</i> -block + L-homo	20.9 ± 10.9	45.5

organosilicate nanostructures templated with the mixture of the D-block and L-block show the presence of three distinct morphologies, contiguous nanoporous films, linear wormlike features, and isolated toroids (Figure 1c–e). The resulting morphologies of organosilicate nanostructures depend on solution concentration and composition. Isolated toroids predominate for all compositions at very low concentrations (≤ 0.1 wt %), while contiguous nanoporous films form at higher concentrations (≥ 1.5 wt %). At intermediate concentrations ($\sim 0.1 < C < \sim 1.5$ wt %), linear wormlike features are observed to coexist with toroids or nanoporous films. The structural similarity of linear features with the others, that is, the internal and outer widths of their channels/voids, suggests that the linear features form by fusion of toroids as an intermediate stage, as detailed in our previous work.³²

The toroids and related nanostructures are also observed in the others with *rac*-block, D-block, and L-block, although the threshold of the morphological transition depends on the types of block copolymers used in the micelle templation. At a high concentration ($C = 2.0$ wt %), the optically pure polylactides, that is, D-block or L-block, form contiguous nanoporous layer structures with the same size and shape as that of *rac*-block in the selected solvent (see Figure S2 in the Supporting Information). However, the mixture of D-block and L-block shows an increase in the vertical height of the nanopores compared those of the racemic or optically pure block copolymers while retaining a similar morphology of contiguous nanoporous films at this concentration. A clear difference between the D-block/L-block mixture and *rac*-block is observed in images of samples made at low concentrations (≤ 0.05 wt %), as shown in Figure 2. The mixture of enantiomers shows morphologies of isolated toroids with the same pore size as that from PDMA-*rac*-PLA. If compared to the racemate, the height of toroids from the D-block/L-block mixtures increases ($\sim 3\times$), while the surface density of toroids decreases. Table 1 summarizes the results of their height distributions and surface coverages calculated from statistical analysis of a *z*-height distribution and image analysis of corresponding AFM photos (see Figures S4 and S5 in the Supporting Information). When block copolymer/organosilicate micelles are deposited, they are flattened and presumably de-wet to expose polylactide core. Toroidal inorganic nanostructures are generated after heating (450 °C). Toroids with a constant difference in heights could be observed in the D-block/L-block mixture, suggesting that 2, 3, 4, ... micelles stack on top of each other, although further studies for full understanding are underway

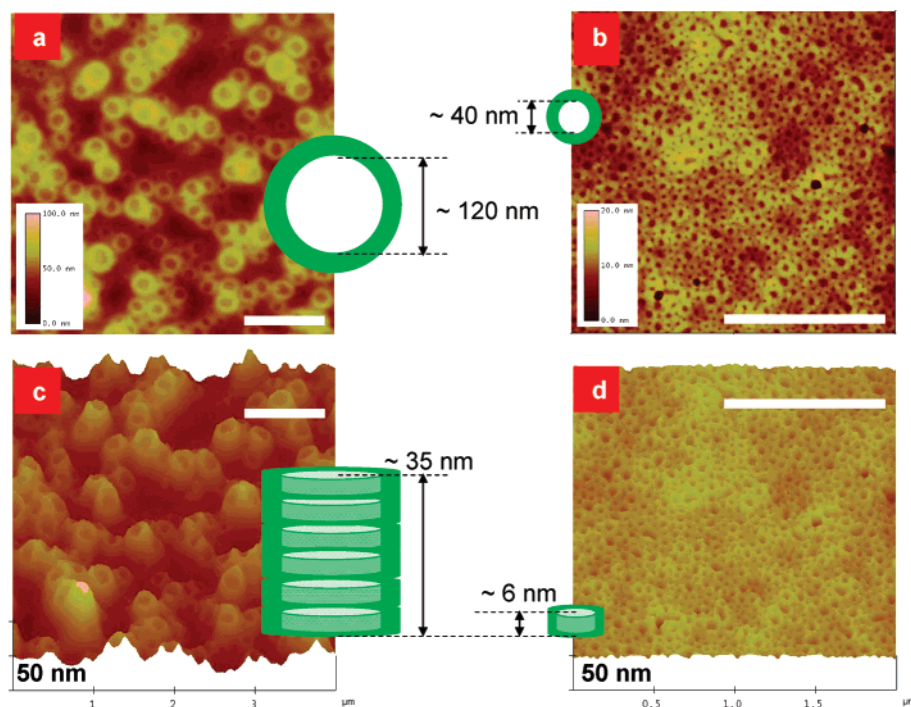


Figure 3. AFM images of organosilicate nanostructures prepared from 2.0 wt % mixtures of block copolymers and homopolymers: (D-block + L-homo)/OS (60/40) (a,c) and (*rac*-block + *rac*-homo)/OS (60/40) (b,d). The stereocomplexation between D-block and L-homo causes the horizontal swelling and vertical growth in their toroidal structure. The scale bars are 1 μ m.

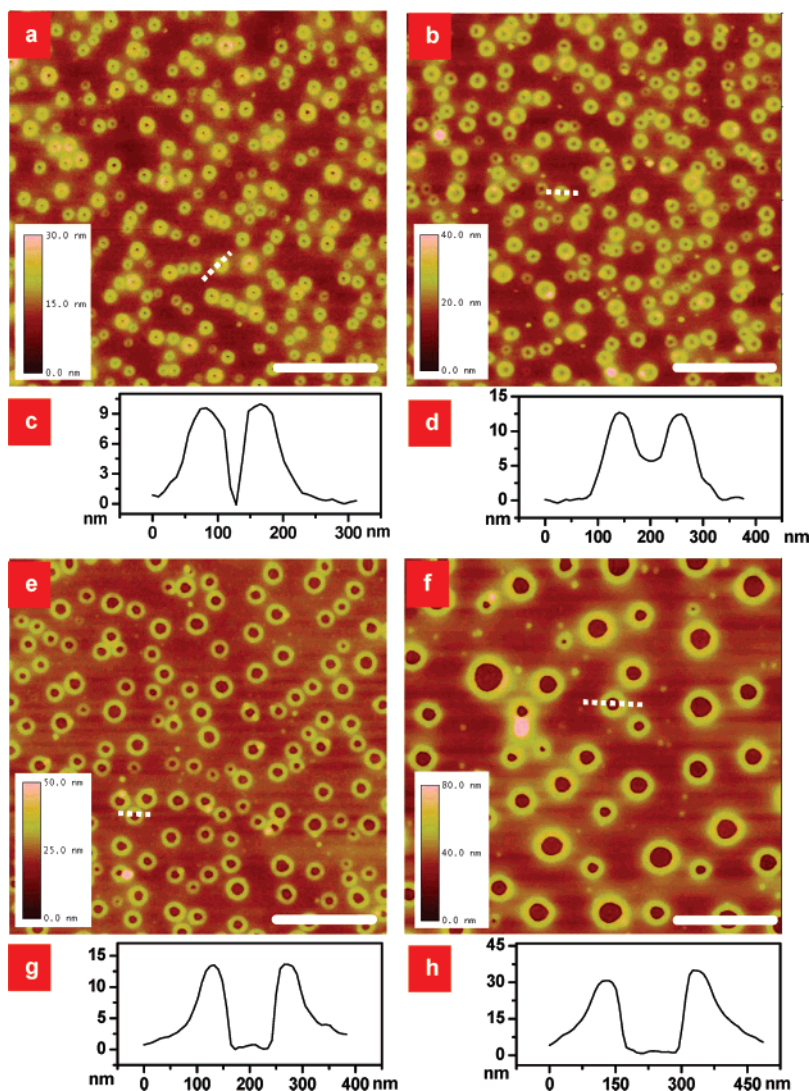


Figure 4. Height contrast AFM images and cross sections of toroids prepared from mixtures of D-block with L-homo of 0.5 (a,c), 1.0 (b,d), 1.5 (e,g), and 2.0 wt % concentrations (f,h) in the D-block (0.05 wt %)/L-homo/OS(2.0 wt %) = 30/30/40 mixtures. Tunable sizes of toroids were obtained by simply increasing the concentration of L-homo. The scale bars are 1 μm .

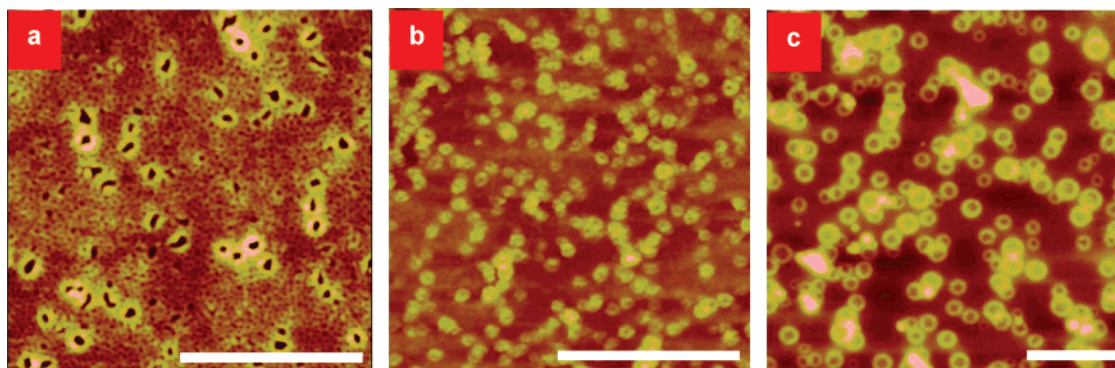


Figure 5. AFM images of inorganic nanostructures obtained from stereoblock PDMA-*sb*-PLA ((a) 2.0 and (b) 0.05 wt % *sb*-block/OS = 60/40), and (c) the mixture with L-homo (2.0 wt % *sb*-block/L-homo/OS = 30/15/60). The scale bars are 1 μm .

(see Figure S6 in the Supporting Information). This indicates that the stereocomplexation between the D-block and L-block induces a preferential deposition and stacking of smaller-unit toroidal micelles, leading to vertical growth of the resulting inorganic toroidal structures while maintaining the

size and shape of core-shell micelles of the block copolymer and organosilicate.

When the stereoregular D-blocks or L-blocks were mixed with the stereocomplementary homopolymer, a significant perturbation in the core-shell dynamic was observed due

to selective swelling of the PLA core owing to stereocomplexation. Figure 3 shows the result of the addition of L-homo into a D-block/organosilicate mixture, where both horizontal swelling and vertical growth of the toroidal structures were observed and attributed to the formation of an intermolecular complex, that is, stereocomplexation (Table 1). This distinctive change does not happen to the mixture of *rac*-block with *rac*-homo (see Figure S3 in the Supporting Information). The stereocomplexation between D-block and L-homo produces different sizes of toroids in diameter from 100 to several hundred nanometers simply by varying the concentration and mixing ratio of L-homo to D-block, as shown in Figure 4 (see Figure S6 in the Supporting Information). Clearly tunable sizes of assembled morphologies are possible by exploiting stereocomplexation between enantiomeric stereopairs.

A stereoblock PLA copolymer (PDMA-*sb*-PLA) that consists of relatively short L-PLA and D-PLA segments in a blocky manner was investigated because the stereoblock PLAs stereocomplex without the addition of a second copolymer or homopolymer. The coassembly of the PDMA-*sb*-PLA with organosilicate under similar preparation conditions also forms toroids at a low concentration of 0.05 wt %, where their size and shape are similar to those of the stereoregular D- or L-block polymers. Horizontal swelling and vertical growth of the toroidal structures were also observed in the mixture of the *sb*-block with the stereoregular homopolymer. One of the differences is that the 2 wt % of PDMA-*sb*-PLA/OS in the selective solvent system shows the formation of not only a nanoporous layer structure but also primitive toroids and linear wormlike morphologies with a horizontal swelling and vertical growth, which may be attributed to the enhanced interaction by the neighboring two blocks of the block copolymer (Figure 5).

In summary, effects of the stereochemistry and stereocomplexation of enantiomeric PLAs on the templation of inorganic nanostructures were investigated via coassembly of an organosilicate precursor with enantiomeric PDMA-PLA block copolymers, PLA homopolymer, and PDMA-*sb*-PLA block copolymers. Exploiting the noncovalent assembly of D- and L- stereocomplexes expands the scope of possible morphological control of block copolymers, providing supramolecular structures with a hierarchical order, as characterized by the distinctive vertical and horizontal growth of toroidal nanostructured inorganic features. The additional control this strategy provides is expected to enhance the refinement of functional materials suitable either for a low-dielectric insulating media and etching masks in microelectronics or for material encapsulation and macromolecular assemblies to transport and deliver biologically active agents.

Acknowledgment. This research was supported by the NSF Center for Polymer Interface and Macromolecular Assemblies (CPIMA: NSF-DMR-0213618). F.N. thanks the Swedish research council (VR) for the financial support. We thank Russell C. Pratt for help in preparing this manuscript and Jane E. Frommer for her valuable suggestions regarding the AFM experiment.

Supporting Information Available: Details on the experimental procedure for the synthesis of block copolymers and homopolymers, their general characteristics and morphologies of optically pure polylactides, that is, D-block or L-block, and statistical analysis on the heights and surface coverage of organosilicate nanostructures. This material is available free of charge via the Internet at <http://pubs.acs.org>

References

- (1) Zhang, L.; Eisenberg, A. *J. Am. Chem. Soc.* **1996**, *118*, 3168.
- (2) Cornelissen, J. J. L. M.; Fischer, M.; Sommerdijk, N.; Nolte, R. J. M. *Science* **1998**, *280*, 1427.
- (3) Discher, D. E.; Eisenberg, A. *Science* **2002**, *297*, 967.
- (4) Li, Z.; Kesselman, E.; Talmon, Y.; Hillmyer, M. A.; Lodge, T. P. *Science* **2004**, *306*, 98.
- (5) Pochan, D. J.; Chen, Z.; Cui, H.; Hales, K.; Qi, K.; Wooley, K. L. *Science* **2004**, *306*, 94.
- (6) Geng, Y.; Ahmed, F.; Bhasin, N.; Disher, D. E. *J. Phys. Chem. B* **2005**, *109*, 3772.
- (7) Alexandridis, P.; Lindman, B. *Amphiphilic Block Copolymers: Self-Assembly and Applications*; Elsevier Science: Amsterdam, The Netherlands, 2000.
- (8) Stoykovich, M. P.; Muller, M.; Kim, S. O.; Solak, H. H.; Edward, E. W.; Pablo, J. J.; Nealey, P. F. *Science* **2005**, *308*, 1442.
- (9) Collier, J. H.; Messersmith, P. B. *Annu. Rev. Mater. Res.* **2001**, *31*, 237.
- (10) Savic, R.; Luo, L. B.; Eisenberg, A.; Maysinger, D. *Science* **2003**, *300*, 615.
- (11) Lodge, T. P.; Bang, J.; Li, Z.; Hillmyer, M. A.; Talmon, Y. *Faraday Discuss.* **2005**, *128*, 1.
- (12) Cui, H.; Chen, Z.; Wooley, K. L.; Pochan, D. J. *Macromolecules* **2006**, *39*, 6599.
- (13) Chen, Z.; Cui, H.; Hales, K.; Li, Z.; Qi, K.; Pochan, D. J.; Wooley, K. L. *J. Am. Chem. Soc.* **2005**, *127*, 8592.
- (14) He, Y.; Li, Z.; Simone, P.; Lodge, T. P. *J. Am. Chem. Soc.* **2006**, *128*, 2745.
- (15) Lee, A. S.; Butun, V.; Vamvakaki, M.; Armes, S. P.; Pople, J. A.; Gast, A. P. *Macromolecules* **2002**, *35*, 8540.
- (16) Petrak, K. *Polyelectrolytes*; Dekker: New York, 1992.
- (17) Chen, D.; Jiang, M. *Acc. Chem. Res.* **2005**, *38*, 494.
- (18) Laiho, A.; Ras, R. H. A.; Valkama, S.; Ruokolainen, J.; Osterbacka, R.; Ikkala, O. *Macromolecules* **2006**, *39*, 7648.
- (19) Ikada, Y.; Jamshidi, K.; Tsuji, H.; Hyon, S.-H. *Macromolecules* **1987**, *20*, 904.
- (20) Tsuji, H. *Macromol. Biosci.* **2005**, *5*, 569.
- (21) Fukushima, K.; Kimura, Y. *Polym. Int.* **2006**, *55*, 626.
- (22) Fukushima, K.; Sogo, K.; Miura, S.; Kimura, Y. *Macromol. Biosci.* **2004**, *4*, 1021.
- (23) Uhrich, K. E.; Cannizzaro, S. M.; Langer, R. S.; Shakesheff, K. M. *Chem. Rev.* **1999**, *99*, 3181.
- (24) Jeong, B.; Bae, Y. H.; Lee, D. S.; Kim, S. W. *Nature* **1997**, *388*, 860.
- (25) Zalusky, A. S.; Olayo-Valles, R.; Wolf, J. H.; Hillmyer, M. A. *J. Am. Chem. Soc.* **2002**, *124*, 12761.
- (26) Rzaev, J.; Hillmyer, M. A. *J. Am. Chem. Soc.* **2005**, *127*, 13373.
- (27) Zhang, J.; Tashiro, K.; Tsuji, H.; Domb, A. J. *Macromolecules* **2007**, *40*, 1049.
- (28) Sarasua, J.-R.; Rodriguez, N. L.; Arraiza, A. L.; Meaurio, E. *Macromolecules* **2005**, *38*, 8362.
- (29) Kang, N.; Perron, M.-E.; Prud'homme, R. E.; Zhang, Y.; Gaucher, G.; Leroux, J.-C. *Nano Lett.* **2005**, *5*, 315.
- (30) Sun, L.; Ginorio, J. E.; Zhu, L.; Sics, I.; Rong, L.; Hsiao, B. S. *Macromolecules* **2006**, *39*, 8203.
- (31) Sun, L.; Zhu, L.; Rong, L.; Hsiao, B. S. *Angew. Chem., Int. Ed.* **2006**, *45*, 7373.
- (32) Choi, J.; Hermans, T. M.; Lohmeijer, B. G. G.; Pratt, R. C.; Dubois, G.; Frommer, J.; Waymouth, R. M.; Hedrick, J. L. *Nano Lett.* **2006**, *6*, 1761.
- (33) Hermans, T. M.; Choi, J.; Lohmeijer, B. G. G.; Dubois, G.; Pratt, R. C.; Kim, H.-C.; Waymouth, R. M.; Hedrick, J. L. *Angew. Chem., Int. Ed.* **2006**, *45*, 6648.
- (34) Chujo, Y.; Saegusa, T. *Adv. Polym. Sci.* **1992**, *100*, 11.
- (35) Huang, Q. R.; Volksen, W.; Huang, E.; Toney, M.; Frank, C. W.; Miller, R. D. *Chem. Mater.* **2002**, *14*, 3676.

- (36) Huang, Q. R.; Kim, H.-C.; Huang, E.; Mecerreyes, D.; Hedrick, J. L.; Volksen, W.; Frank, C. W.; Miller, R. D. *Macromolecules* **2003**, *36*, 7661.
- (37) Chamberlain, B. M.; Cheng, M. C.; Moore, D. R.; Ovitt, T. M.; Lobkovsky, E. B.; Coates, G. W. *J. Am. Chem. Soc.* **2001**, *123*, 3229.
- (38) Ovitt, T. M.; Coates, G. W. *J. Am. Chem. Soc.* **2002**, *124*, 1316.
- (39) Hawker, C. J.; Bosman, A. W.; Harth, E. *Chem. Rev.* **2001**, *101*, 3661.
- (40) Zhang, L.; Nederberg, F.; Messman, J. M.; Pratt, R. C.; Hedrick, J. L.; Wade, C. G. *J. Am. Chem. Soc.* **2007**, *129*, 12610.
- (41) Yui, N.; Dijkstra, P. J.; Feijen, J. *J. Makromol. Chem.* **1990**, *191*, 481.
- (42) Kricheldorf, H. R.; Rost, S.; Wutz, C.; Domb, A. *Macromolecules* **2005**, *38*, 7018.

NL0726813